glass flasks that have been prefilled and shipped with clean, dry air. For the ships, evacuated flasks are exposed to air. Potential offsets between these two sampling methods are still under investigation.
23. P. J. Crutzen and M. O. Andreae, *Science* **250**, 1669 (1990). The burning of savannas in North Africa occurs essentially from December to March. It could be followed by the decomposition of organic matter in soils during the next rain season from April to July (H. Cachier, personal communication).
24. F. Joos, P. Ciais, L. Currie, in "Isotope Variation of Carbon Dioxide and Other Trace Gases in the Atmosphere," K. Rozanski, Ed. [final report on the International Atomic Energy Agency (IAEA) Coordinated Research Program, IAEA, Vienna, Austria, 1995].
25. We thank P. Gemery, D. Young, C. Brock, D. Bryant, D. Decker, and S. Webb for making the isotopic analyses. T. Conway and N. Zhang were responsible for the analyses of CO_2 and L. Waterman for the logistics of the flask network. We are grateful to the many individuals and organizations who contributed to the NOAA/CMDL cooperative flask sampling network. The Cape Grim Baseline Air Pollution Station, the Australian Antarctic Division, and CSIRO's GASLAB assisted in the provision of Southern Hemisphere results. K. Masarie contributed to the data management of $\delta^{13}C$. Partial support was provided by the Ocean Atmosphere Carbon Exchange Study and the Atmospheric Chemistry projects of the Climate and Global Change Program of NOAA and by the Atmospheric Research and Exposure Assessment Laboratory of the Environmental Protection Agency.

13 February 1995; accepted 12 June 1995

Similarity of *sli-1*, a Regulator of Vulval Development in *C. elegans*, to the Mammalian Proto-Oncogene c-*cbl*

Charles H. Yoon, Junho Lee, Gregg D. Jongeward, Paul W. Sternberg*

Vulval induction during *Caenorhabditis elegans* development is mediated by LET-23, a homolog of the mammalian epidermal growth factor receptor tyrosine kinase. The *sli-1* gene is a negative regulator of LET-23 and is shown here to encode a protein similar to c-Cbl, a mammalian proto-oncoprotein. SLI-1 and c-Cbl share approximately 55 percent amino acid identity over a stretch of 390 residues, which includes a C_3HC_4 zinc-binding motif known as the RING finger, and multiple consensus binding sites for Src homology 3 (SH3) domains. SLI-1 and c-Cbl may define a new class of proteins that modify receptor tyrosine kinase–mediated signal transduction.

The induction of the vulva in *Caenorhabditis elegans* provides a model system in which to apply genetic analysis in order to dissect proto-oncogene function (*1*). Vulval induction is mediated by LET-23, a homolog of the epidermal growth factor receptor tyrosine kinase; by SEM-5, a Grb2-like adaptor; and by LET-60, a Ras protein (*2–4*). Genetic analyses have identified negative regulators of this pathway. Thus, the *sli-1* (suppressor of lineage defect) locus was defined by extragenic suppressors of *let-23* reduction-of-function (*rf*) mutations (*5*). The *let-23(rf)* mutations cause at least five phenotypes: defects in (i) viability, (ii) hermaphrodite fertility, (iii) male spicule development, (iv) posterior epidermal development, and (v) vulval differentiation (6). The *sli-1(rf)* mutations suppress all known defects of *let-23(rf)* mutations with the exception of sterility. For example, the *sli-1(sy143)* mutation restores vulval induction to wild type in animals with *let-23(sy97)*, a severe reduction-of-function allele that truncates a part of the LET-23 cytoplasmic tail and results in a vulvaless (Vul) phenotype (6). *sli-1* does not, however, bypass the requirement for *let-23* because *sli-1(rf)* mutations do not suppress *let-23* null alleles, which are lethal.

Reduction-of-function mutations in *sem-5* and *let-60* also display Vul phenotypes, and the products of these genes act downstream in a signal transduction process initiated by LET-23 (*3, 4*). The *sli-1(sy143)* mutation suppresses the Vul phenotype associated with a weakly hypomorphic *sem-5(n2019)* to near, but not greater than, wild type; *sli-1(sy143)* also weakly suppresses a very weak *let-60(rf)* mutation, *n2021* (*5*). Lethality associated with *let-60(s1124)*, a severe hypomorph, is not suppressed by *sli-1(sy143)* (*5*), which suggests that the *sli-1(rf)* mutation does not bypass the requirement for LET-60.

Although *sli-1(rf)* mutations alone are silent in a *let-23(+)* background, in combination with a mutation in another silent negative regulator of LET-23–mediated vulval development, *unc-101*, a *sli-1(rf)* mutation displays a multivulva (Muv) phenotype (*7*). Therefore, SLI-1 can act on signaling by wild-type LET-23.

We have now identified *sli-1* at the molecular level by positional cloning. Three-factor mapping positioned *sli-1* midway between *egl-17* and *unc-1*, which are about one map unit apart on the extreme left end of the *C. elegans* X chromosome (Fig. 1A) (*5*). The restriction fragment length polymorphism (RFLP) *stP41* links the genetic and physical maps in this region: *stP41* is tightly linked to *unc-1* and thus defines the right boundary of our region of interest (*8*). Assuming that the left boundary is the left end of the X chromosome, *sli-1* lies in the middle of a region spanned by ~40 cosmids (9). To assay for *sli-1(+)* wild-type activity, we used a sensitive vulva-specific *let-23(rf)* allele, *sy1*. Whereas *let-23(sy1)* is Vul (Fig. 2B), *let-23(sy1); sli-1(sy143)* animals have a Muv phenotype (Fig. 2C). We microinjected candidate cosmids from the middle of the genomic region of interest into the germ line of the *let-23(sy1); sli-1(sy143)* parental strain and observed the vulval phenotype of stably transformed progeny in F_2 or later generations (*10*). Microinjection of the cosmid T18D5 rescued the Muv phenotype of *let-23(sy1); sli-1(sy143)* double mutants, and stable germ line–transformed progeny showed the Vul phenotype typical of *let-23(sy1)* strains (Fig. 1A and Fig. 2, B and D). Other cosmids in the region (F02G3, F25H6, and F25E2) did not rescue the Muv phenotype of the *let-23(sy1); sli-1(sy143)* parent strain. T18D5 also rescued the Muv phenotype of another *sli-1* allele, *sy129*, in our assay, which indicates that this cosmid contains the wild-type activity of *sli-1*.

We tested subclones of the 35-kb genomic insert of T18D5 to localize the region responsible for rescuing activity. A 16-kb Eco RV–Nhe I subclone (pSli1.16) and a 10-kb Eco RV–Nhe I subclone (pSli1.10) retained the rescuing activity of T18D5 (Fig. 1B and Table 1). Thus, these two subclones contain the wild-type *sli-1* gene; the smaller pSli1.10 is contained within the larger pSli1.16.

We isolated complementary DNAs (cDNAs) by probing the Barstead cDNA library with a 9-kb genomic fragment that overlaps pSli1.10 (*11*). One cDNA was 2.2 kb in length and is likely to be full length, because it includes the last nine base pairs of the SL1 trans-spliced leader sequence at the 5′ end. We also identified one class of alternatively spliced cDNA. We sequenced the full-length 2.2-kb cDNA, the longest available alternatively spliced cDNA, and the genomic fragment in pSli1.10. The open reading frame of the 2.2-kb cDNA encodes a putative translation product of 582 amino acids. The genomic structure of *sli-1* consists of 11 exons and 10 introns, spanning 6 kb in

C. H. Yoon and P. W. Sternberg, Howard Hughes Medical Institute and Division of Biology, California Institute of Technology, Pasadena, CA 91125, USA.
J. Lee, Department of Molecular and Cell Biology, University of California, Berkeley, CA 94720, USA.
G. D. Jongeward, Department of Microbiology, Immunology, and Biochemistry, University of California, San Francisco, CA 94143-0502, USA.
*To whom correspondence should be addressed.

length (Fig. 1B), and the entire genomic coding sequence lies within pSli1.10. The alternatively spliced cDNA lacks exon 10, and its 5′ end extends into exon 5.

Identification of the molecular lesions associated with *sy143* and *sy129* alleles confirmed that the full-length transcript corresponds to the *sli-1* locus (Fig. 3A) (*12*). *sy143* is an amber mutation in exon 5 and presumably results in the production of a nonfunctional protein that lacks the COOH-terminal 74% of SLI-1. This early stop codon is consistent with genetic tests that suggest that *sy143* severely reduces *sli-1(+)* function (*5*). *sy129*, also a strong reduction-of-function allele (*5*), is a missense mutation that changes Gly^{315} to Glu.

Searches of the GenBank and SWISS-PROT databases revealed that the inferred sequence of SLI-1 is highly similar to that of the product of a mammalian proto-oncogene, c-*cbl* (Fig. 3, A and B) (*13*). The *cbl* gene was originally identified in the murine Cas NS-1 retrovirus as v-*cbl*, an acute oncogene that induces progenitor B cell, precursor B cell, and myeloid tumors in mice (*14*, *15*). c-*cbl*, the cellular version of v-*cbl*, has been identified in both humans and mice (*14*). Human c-Cbl contains 906 amino acids and is located in the cytoplasm. Two oncogenic forms of Cbl have been identified: a COOH-terminal truncation of c-Cbl that produces v-Cbl (Fig. 3B) (*15*) and a form with an internal deletion of 17 residues (*16*).

The alignment of SLI-1 to c-Cbl reveals several shared domains (Fig. 3B) (*17*). A stretch of 390 amino acids in SLI-1 (residue 58 to 447) shows ~55% sequence identity to c-Cbl. The *sy129* $Gly^{315} \rightarrow$ Glu substitution lies in the middle of this stretch and affects a conserved

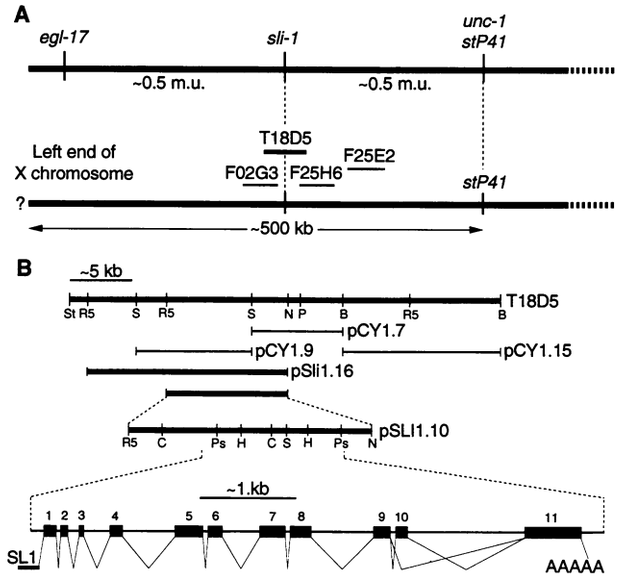

Fig. 1. Positional cloning of *sli-1*. (**A**) Genetic and physical maps of the extreme left end of the *C. elegans* X chromosome (*9*). The RFLP *stP41* links the genetic (upper) and physical (lower) maps near the *unc-1* locus (*8*). *sli-1* lies midway between *egl-17* and *unc-1* (*5*). Whereas *let-23(sy1); sli-1(sy143)* double mutants have a Muv phenotype, *let-23(sy1)* single mutants are Vul. The cosmid T18D5 rescues the *sli-1(rf)* defect and thus confers a Vul phenotype on germ line–transformed progeny derived from *let-23(sy1); sli-1(sy143)* parents (*10*). Cosmids F02G3, F25H6, and F25E2 do not show *sli-1* rescuing activity; m.u., map units. (**B**) Partial restriction map of T18D5 and the genomic structure of *sli-1*. Subclones of T18D5 were tested for *sli-1* rescuing activity (*10*). Both the 16-kb Eco RV–Nhe I (pSli1.16) and the 10-kb Eco RV–Nhe I (pSli1.10) subclones maintain *sli-1* rescuing activity, whereas other subclones (pCY1.9, pCY1.7, and pCY1.15) do not. pSli1.10 is enlarged to show a partial restriction map. Dotted lines from pSli1.10 to the *sli-1* genomic structure indicate the region of *sli-1* within the subclone. The *sli-1* genomic structure is derived from cDNA and genomic sequences. At least one alternatively spliced cDNA was isolated; it lacks exon 10 of the full-length transcript. SL1 denotes the SL1 trans-spliced leader sequence. B, Bgl I; C, Cla I; H, Hind III; N, Nhe I; P, Pvu I; Ps, Pst I; R5, Eco RV; S, Sal I; St, Stu I.

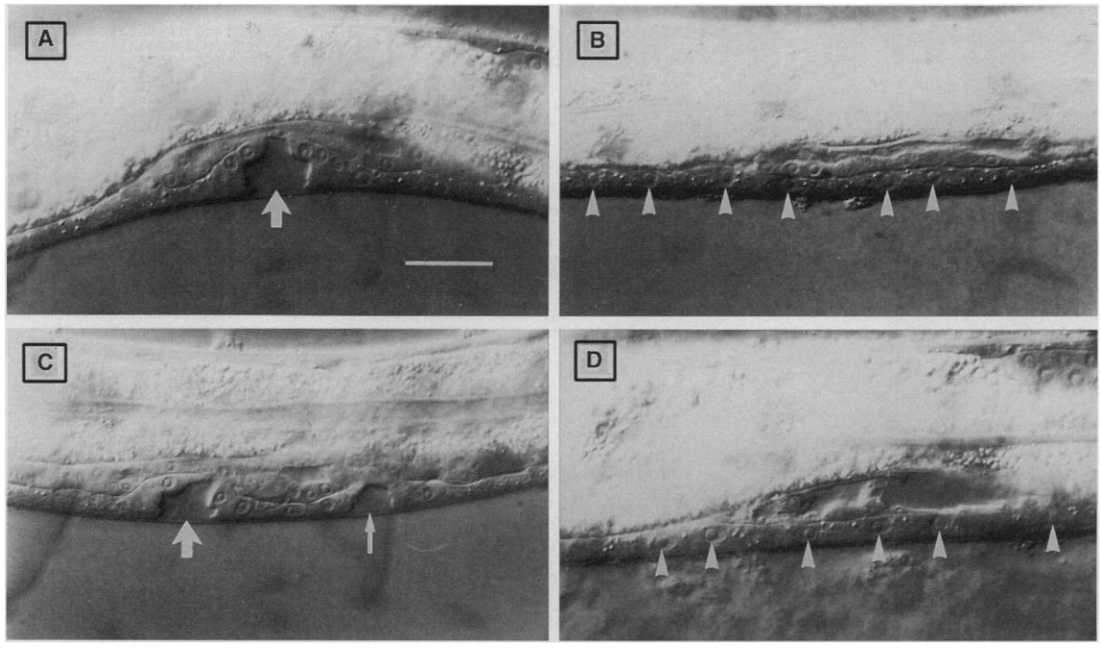

Fig. 2. Vulval differentiation in *sli-1* genotypes (*10*, *25*). (**A**) Wild type: N2 strain. Arrow indicates the wild-type vulva, which is derived from three of six vulval precursor cells (VPCs). (**B**) Vul: *let-23(sy1); dpy-20(e1282); syEx[pSK+, pMH86(dpy-20(+))]* strain. All daughters of the six VPCs have nonvulval epidermal fates. Arrowheads indicate epidermal nuclei derived from VPC daughters. The Vul phenotype of this non-Dpy transgenic marker strain is the same as that observed in *let-23(sy1)* strains. (**C**) Muv: *let-23(sy1); sli-1(sy143)*. The fat arrow indicates a nearly normal vulva that will open into the uterine cavity. The thin arrow indicates an extra pseudo-vulva; more than three VPCs have acquired vulval fates. The Muv phenotype is unaffected in transgenic marker strains such as *let-23(sy1); sli-1(sy143); syEx[pRF4(rol-6(su1006))]* and *let-23(sy1); dpy-20(e1282); sli-1(sy143); syEx[pMH86(dpy-20(+))]*. (**D**) Vul *let-23(sy1); unc-31(e169); sli-1(sy143); syEx[T18D5, C14G10(unc-31(+))]* animal. Arrowheads indicate epidermal nuclei. All six VPCs produce daughters with epidermal fates; the phenotype is the same as that observed in *let-23(sy1)* (B). Thus, the cosmid T18D5 shows *sli-1* rescuing activity, which is maintained in strains with Rol and non-Dpy transgenic markers. Scale bar in (A), 20 μm; same scale for all panels. Ventral side is down and anterior is to the left in all panels.

residue in a region of ~80% (16/21) amino acid identity between SLI-1 and c-Cbl. The COOH-terminal end of this conserved region constitutes a RING finger, a putative zinc-binding C_3HC_4 motif distinct from the classic zinc finger (*18*). The RING finger regions of SLI-1 and c-Cbl share 70% (45/64) identity (Fig. 3A). The transforming activity of Cbl does not require the RING finger; the oncogenic forms of Cbl lack part or all of this structure (*14–16*). Because of the genetic interactions of *sli-1* with *let-23*, *sem-5*, and *let-60*, as well as the sequence similarity of SLI-1 to the cytoplasmically localized c-Cbl (*19*), we favor models in which SLI-1 interacts directly with other proteins in the signal transduction pathway. The RING finger may play a structural role required for SLI-1 wild-type function or interactions with other proteins, or both.

The COOH-terminal region of SLI-1 contains three potential Src homology 3 (SH3)–binding motifs with conserved proline residues (Fig. 3) (*20*, *21*). These proline domains are similar to the SH3-binding motifs of proteins such as murine 3BP1 and Sos1, and *Drosophila* Sos (*20*, *21*). SH3 domains are present in many proteins that participate in signal trans-

Table 1. Vulval differentiation of *let-23*, *sli-1*, and transgenic genotypes (*25*). pSli1.16 rescues the suppressor phenotype of *sli-1*(*sy143*) to restore wild-type or multivulva animals to vulvaless (*10*).

Genotype			Vulval phenotype*			
let-23	*sli-1*	Injected DNA†	Differentiated VPCs per animal	Vul (%)	Muv (%)	Animals (*n*)
+	+	–	3.0	0	0	32
sy1	+	–	0.3	80	0	45
sy1	*sy143*	–	3.6	0	68	25
+	+	pSli1.16	3.04	0	2	42
sy1	+	pSli1.16	0.12	92	0	50
sy1	*sy143*	pSli1.16	0.9	69	9.4	32

*Vulval differentiation as scored by Nomarski optics. 1° and 2° VPC fates are scored as differentiated. In each wild-type animal, three of six VPCs underwent vulval differentiation. Vul phenotype indicates no differentiated VPCs. Muv phenotype indicates more than three differentiated VPCs per animal. Differentiation scores are averaged for the number of animals scored (*n*) for a given genotype (row). †All *let-23* and *sli-1* genotypes are scored in germline-transformed animals [non-Dpy from *dpy-20*(*e1282*) background] (*10*). Dpy-20 transgenic marker (pMH86) was injected at 15 ng/μl, except in the first row, in which it was injected at 10 ng/μl. Dash indicates carrier DNA: In the first row, pSK+ (100 ng/μl) and pJMG3BP.11 (50 ng/μl) were injected with pMH86; in the second and third rows, pSK+ plasmid (150 ng/μl) was injected with pMH86. pSli1.16 indicates the 16-kb *sli-1* rescuing fragment (150 ng/μl) injected with pMH86.

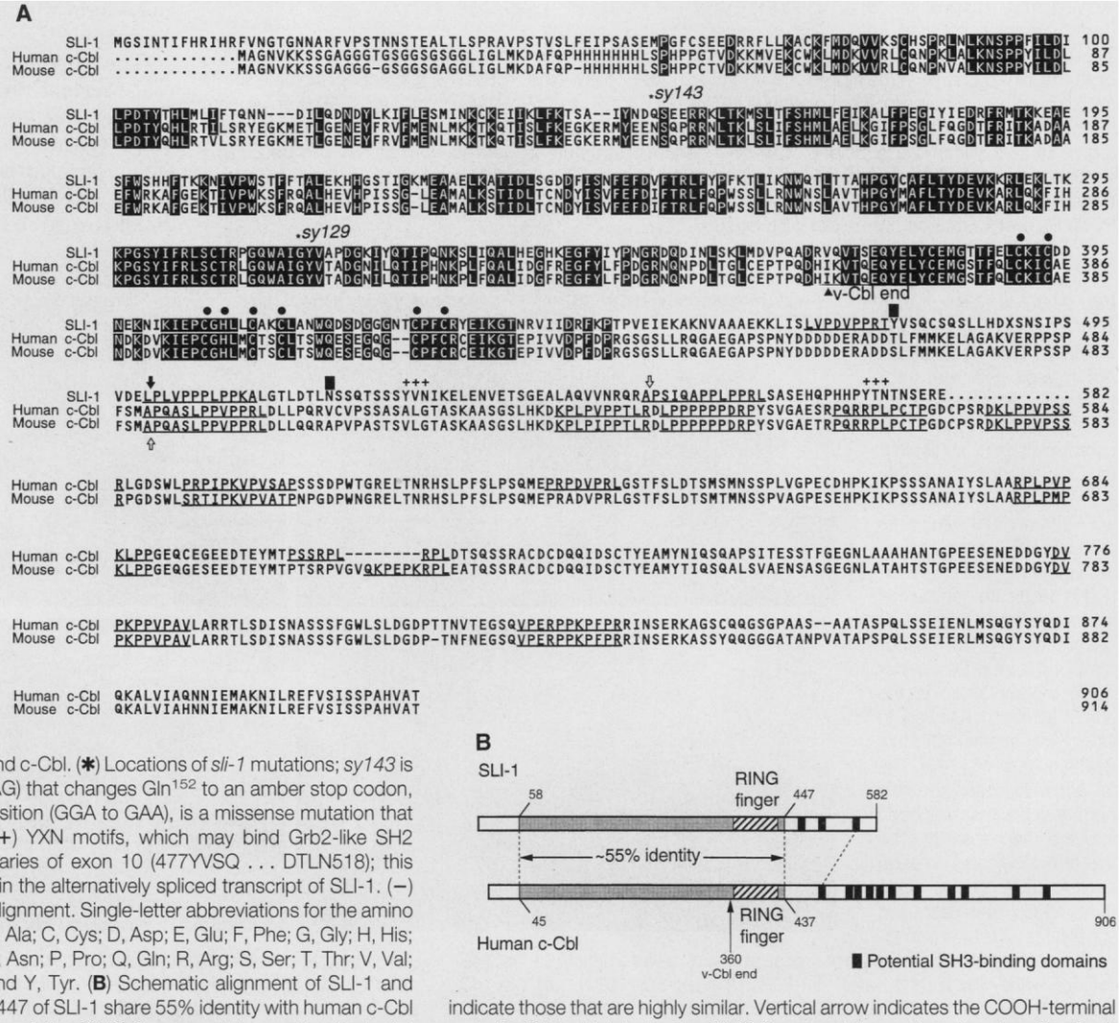

Fig. 3. Comparison of SLI-1 and mammalian c-Cbl proteins. (**A**) Alignment of the inferred SLI-1 protein sequence to those of human and mouse c-Cbl (*17*). Identical amino acid residues between SLI-1 and c-Cbl are highlighted in black. The last amino acid residue of each row is numbered. (▲) The COOH-terminal end of v-Cbl; QDHI in c-Cbl is replaced by HF-Samber in v-Cbl. (●) The conserved C_3HC_4 motif of the RING finger (*18*). Potential SH3-binding motifs with conserved prolines (proline domains) (*20*, *21*) are underlined in SLI-1 and in human and mouse c-Cbl. There are three distinct proline domains in SLI-1; human and mouse c-Cbl contain 11 and 10 proline domains, respectively. (↓) The SLI-1 proline domain similar to that present in murine 3BP1 (*20*); (⇦ and ⇦) proline domains that are highly similar between SLI-1 and c-Cbl. (✱) Locations of *sli-1* mutations; *sy143* is a C → T transition (CAG to TAG) that changes Gln^{152} to an amber stop codon, whereas *sy129*, a G → A transition (GGA to GAA), is a missense mutation that changes Gly^{315} to Glu. (+++) YXN motifs, which may bind Grb2-like SH2 domains (*24*). (■) The boundaries of exon 10 (477YVSQ . . . DTLN518); this stretch of residues is missing in the alternatively spliced transcript of SLI-1. (–) Gaps introduced to optimize alignment. Single-letter abbreviations for the amino acid residues are as follows: A, Ala; C, Cys; D, Asp; E, Glu; F, Phe; G, Gly; H, His; I, Ile; K, Lys; L, Leu; M, Met; N, Asn; P, Pro; Q, Gln; R, Arg; S, Ser; T, Thr; V, Val; W, Trp; X, any amino acid; and Y, Tyr. (**B**) Schematic alignment of SLI-1 and human c-Cbl. Residues 58 to 447 of SLI-1 share 55% identity with human c-Cbl residues 45 to 437. Positions of the RING finger and the proline (potential SH3-binding) domains are shown. Dotted lines linking two proline domains indicate those that are highly similar. Vertical arrow indicates the COOH-terminal end of v-Cbl, which lacks the RING finger and the proline domains. GenBank accession number is X89223.

duction (22), and SLI-1 may physically interact with such proteins through its SH3-binding domains. Functional significance of the second SLI-1 proline domain is further suggested by its location in exon 10, which is missing in the alternatively spliced form of the protein (Figs. 1B and 3A).

There are 11 potential SH3-binding domains in human c-Cbl and 10 in the mouse protein (Fig. 3). Indeed, the COOH-terminal portion of c-Cbl, including the proline domains, can bind SH3 domains of $p47^{nck}$, a signaling adaptor, in vitro, and c-Cbl binds to Grb2/Ash in vivo and in vitro (23). The proline domains lie in a region that shows no overall sequence similarity between SLI-1 and c-Cbl, and the domains themselves are divergent in sequence; however, one of the c-Cbl proline domains closely resembles one of the SLI-1 proline domains.

Near the proline-rich domains, SLI-1 contains two YXN motifs (Fig. 3A). Grb2-like SH2 domains preferentially bind phosphorylated tyrosine residues in YXN peptides (24). Thus, SLI-1 also may interact with signaling proteins through these potential SH2-binding domains. c-Cbl, however, does not have YXN motifs near its proline domains. The lack of the YXN motif in c-Cbl and the differing number and configuration of the putative SH3-binding domains in SLI-1 and c-Cbl suggest some divergence between the regulators or targets of these two proteins.

It is possible that SEM-5 is the major target of SLI-1 action. The SLI-1 proline-rich domains and YXN motifs may bind to the SEM-5 SH3 and SH2 domains, respectively, and prevent SEM-5 from transducing the LET-23 signal and activating Ras. It is also possible that SLI-1 regulates the LET-23 pathway through other general mechanisms such as protein degradation. However, the suppression of *let-23(sy97)* by *sli-1(rf)* mutations and the molecular lesion associated with the *sy97* allele suggest additional models. As a result of the truncation of part of the cytoplasmic tail, $LET\text{-}23^{sy97}$ lacks tyrosine residues that are proposed to serve as binding sites for SEM-5 in the wild-type protein (6); thus, the *sy97* lesion may decouple LET-23 from the SEM-5 pathway. There are two simple mechanisms by which *sli-1(rf)* mutations might restore signaling to $LET\text{-}23^{sy97}$. First, SLI-1 might interact directly with LET-23 and normally restrict SEM-5 binding to specific sites in the LET-23 cytoplasmic tail; elimination of SLI-1 might then allow SEM-5 to bind other tyrosine residues in the remaining cytoplasmic region of $LET\text{-}23^{sy97}$. Second, SLI-1 might negatively regulate a pathway independent of SEM-5 activity; elimination of SLI-1 would then allow the alternative pathway to bypass the requirement for SEM-5 activation in *let-23(sy97); sli-1(rf)* double mutants.

Genetic studies and structural domains discussed above suggest that SLI-1 undergoes direct physical interactions with signaling molecules associated with LET-23. Mammalian c-Cbl has not previously been linked to tyrosine kinase and Ras pathways. Although the wild-type function of c-Cbl is unknown, the similarity of c-Cbl to SLI-1 in sequence and overall architecture predicts that c-Cbl acts in mammalian receptor tyrosine kinase–mediated signaling.

REFERENCES AND NOTES

1. P. W. Sternberg, *Annu. Rev. Genet.* **27**, 497 (1993).
2. R. V. Aroian, M. Koga, J. E. Mendel, Y. Ohshima, P. W. Sternberg, *Nature* **348**, 693 (1990).
3. S. G. Clark, M. J. Stern, H. R. Horvitz, *ibid.* **356**, 340 (1992); G. J. Beitel, S. G. Clark, H. R. Horvitz, *ibid.* **348**, 503 (1990).
4. M. Han and P. W. Sternberg, *Cell* **63**, 921 (1990); M. Han, R. V. Aroian, P. W. Sternberg, *Genetics* **126**, 899 (1990).
5. G. D. Jongeward, T. R. Clandinin, P. W. Sternberg, *Genetics* **139**, 1553 (1995).
6. R. V. Aroian, G. M. Lesa, P. W. Sternberg, *EMBO J.* **13**, 360 (1994); R. V. Aroian and P. W. Sternberg, *Genetics* **128**, 251 (1991).
7. Thirteen of 20 *unc-101(sy108); sli-1(sy143)* hermaphrodites showed greater than wild-type vulval differentiation. J. Lee, G. D. Jongeward, P. W. Sternberg, *Genes Dev.* **8**, 60 (1994).
8. A. Villeneuve, personal communication.
9. Cosmids and the physical map data are from A. Coulson and J. Sulston [A. R. Coulson, J. Sulston, S. Brenner, J. Karn, *Proc. Natl. Acad. Sci. U.S.A.* **83**, 7821 (1986); A. R. Coulson, R. Waterston, J. Kiff, J. Sulston, Y. Kohara, *Nature* **335**, 184 (1988)].
10. Germline transformation was performed with several transgenic markers [C. C. Mello, J. M. Kramer, D. Stinchcomb, V. Ambros, *EMBO J.* **10**, 3959 (1991)]. The dominant Rol-6 roller marker (plasmid pRF4 at 50 ng/μl) was co-injected with test DNA in *let-23(sy1); sli-1(sy143)* Muv strains. The Unc-31 rescuing cosmid C14G10 was used at 90 ng/μl in *let-23(sy1); unc-31(e169); sli-1(sy143)* Muv–Unc (uncoordinated) strains. The Dpy-20 rescuing plasmid pMH86 was used at 15 ng/μl in *let-23(sy1); dpy-20(e1282); sli-1(sy143)* Muv–Dpy (dumpy) strains. Test DNA was injected at concentrations of 100 to 150 ng/μl, for a total injected DNA concentration of 150 to 200 ng/μl. Germ line–transformed progeny carried the co-injected marker and test DNA in extrachromosomal arrays, and were identified by roller (Rol), non-uncoordinated (non-Unc), or non-dumpy (non-Dpy) phenotypes in our experiments. F_2 or older populations were scored for vulval phenotypes.
11. The 9-kb genomic clone pCY1.9 was used to screen ~1.6×10^6 plaques from the Barstead cDNA library derived from mixed-stage polyadenylated RNA [R. J. Barstead and R. H. Waterston, *J. Biol. Chem.* **264**, 10177 (1989)]. Three positive clones were isolated that hybridized to the rescuing fragment pSli1.10. The longest clone was then used to rescreen the cDNA library, and 62 positive clones were isolated. All three clones from the first screen and 18 clones from the second screen were fully or partially sequenced with Sequenase v.2.0 (U.S. Biochemical, Cleveland, OH); all clones were identical in sequence with the exception of the extent of their 5′ ends and the alternatively spliced region. cDNA sequences were compiled on MacVector 3.5 (IBI, New Haven, CT). Restriction map analysis was used in conjunction with sequencing to compare cDNAs. The rescuing genomic fragment pSli1.10 was sequenced on both strands with cDNA primers and primers derived from partial genomic sequence.
12. Mutant genomic DNA was amplified by the polymerase chain reaction (PCR); 5 to 10 hermaphrodites in the first and second larval stages were used for each PCR reaction [B. D. Williams, B. Schrank, C. Huynh, R. Shownkeen, R. H. Waterston, *Genetics* **131**, 609 (1992)]. Exons, including exon-intron borders, were amplified with primers located within the introns. Amplification primers were as follows: exons 1 to 6, 5′-GTTGATTCAATTTACCGCCCTC and 5′-CCAATTTGGTCAGTGCTCGCGG; exons 7 to 10, 5′-GTTGCACTGACCAAAATGCTTTC and 5′-CAAAGCAATGCAAAGCATGCAC; exon 11, 5′-CAGCCAAACCCTATATGCGC and 5′-GCGTCGTGCACTTACCAGTTCGC. Amplified fragments were subcloned into the Eco RV site of the pSK+ vector. Each amplification reaction was performed in duplicate, and two separate subclones were chosen from each (thus, four independent subclones per amplified genomic fragment). PCR errors were identified by sequencing of two independent subclones of a given genomic fragment. *sli-1* mutations were confirmed by sequencing of all four independent subclones of a given genomic fragment. The following primers, in addition to those listed above were used for sequencing: 5′-GCAGCCCGATTGGACTTCAGC, 5′-GAAGATTTGCCAAATTGCCCAGG, 5′-TTATCTATTAGCAAGCCCAAGC, 5′-CAAGTCTTTTAGGAAAACAACTGG, 5′-GGTTGCAATGAAGCATTGTGTGC, 5′-GTGCTGGGAACAGCTCTCGG, 5′-GACCAGTCTGAAGAACGACGG, 5′-GCAATAGGATACGTAGCTCC, 5′-AGCTGCTGCGGAGAAGAAGC, 5′-CGAGCACCAACCACACCACC, and 5′-GCTACGATAGACTTGAGCGG.
13. GenBank and SWISS-PROT databases were searched with the BLAST service at the National Center for Biotechnology Information.
14. W. Y. Langdon, J. W. Hartley, S. P. Klinken, S. K. Ruscetti, H. C. Morse III, *Proc. Natl. Acad. Sci. U.S.A.* **86**, 1168 (1989).
15. T. J. Blake, M. Shapiro, H. C. Morse III, W. Y. Langdon, *Oncogene* **6**, 653 (1991).
16. C. E. Andoniou, C. B. F. Thien, W. Y. Langdon, *EMBO J.* **13**, 4515 (1993).
17. Alignment of SLI-1 and c-Cbl was done with Pileup and PrettyPlot programs (Genetics Computer Group, v.7, University of Wisconsin, Madison) and refined by eye. Similarity in proline-rich domains between SLI-1 and c-Cbl was identified by the BLAST search (*13*).
18. P. S. Freemont, *Ann. N.Y. Acad. Sci.* **684**, 174 (1993).
19. T. J. Blake, K. G. Heath, W. Y. Langdon, *EMBO J.* **12**, 2017 (1993).
20. R. Ren, B. J. Mayer, P. Cicchetti, D. Baltimore, *Science* **259**, 1157 (1993); H. Yu *et al.*, *Cell* **76**, 933 (1994).
21. R. Ren, Z.-S. Ye, D. Baltimore, *Genes Dev.* **8**, 783 (1994); J. P. Olivier *et al.*, *Cell* **73**, 179 (1993).
22. T. Pawson and J. Schlessinger, *Curr. Biol.* **3**, 434 (1993); T. Pawson and G. D. Gish, *Cell* **71**, 359 (1992).
23. O. M. Rivero-Lozcano, J. H. Sameshima, A. Marcilla, K. C. Robbins, *J. Biol. Chem.* **269**, 17363 (1994); H. Odai *et al.*, *ibid.* **270**, 10800 (1995).
24. Z. Songyang *et al.*, *Cell* **72**, 767 (1993).
25. Vulval differentiation was scored at L3 molt and early L4 larval stages under Nomarski optics. Culture, handling, and genetic manipulation of *C. elegans* were performed as described [S. Brenner, *Genetics* **77**, 71 (1974)]. Representative specimens were photographed on Kodak Techpan film under Nomarski optics.

26. We thank G. Lesa, N. Hopper, and R. Sommer for comments on the manuscript; G. Medina and other members of the Sternberg laboratory for technical assistance; J. Mendel for pJMG3BP.11; and W. Langdon for discussions. Supported by a grant from the U.S. Public Health Service to P.W.S., who is an investigator with the Howard Hughes Medical Institute.

13 April 1995; accepted 2 June 1995